

Population density modulates insect progenitive plasticity through the regulation of dopamine biosynthesis

Kai Liu

Sun Yat-Sen University

Longyu Yuan

Sun Yat-Sen University

Lei Yue

Sun Yat-Sen University

Weiwen Chen

Sun Yat-Sen University

Kui Kang

Sun Yat-Sen University

Jun Lv

Sun Yat-Sen University

Wenqing Zhang

Sun Yat-Sen University

Rui Pang (✉ pr839@163.com)

Sun Yat-Sen University <https://orcid.org/0000-0001-9300-6142>

Research Article

Keywords: Brown planthopper, Fecundity, Population density, Genotype, Dopamine biosynthesis

Posted Date: February 24th, 2021

DOI: <https://doi.org/10.21203/rs.3.rs-215638/v1>

License: © ⓘ This work is licensed under a Creative Commons Attribution 4.0 International License.

[Read Full License](#)

Version of Record: A version of this preprint was published at Insect Science on March 1st, 2022. See the published version at <https://doi.org/10.1111/1744-7917.13019>.

31 progenitive phenotypes of BPH. This study shows that the dopamine biosynthesis is the key
32 regulatory factor for the determination of fecundity in response to density changes in different
33 genotypes of BPH, which gives an insight into the interaction of a typical environmental
34 factor and insect genotype during the process of population regulation.

35 **Key works:** Brown planthopper · Fecundity · Population density · Genotype · Dopamine
36 biosynthesis

37

38 **Key Message**

- 39 ● The interaction of environment factors and genotypes on the fecundity of the brown
40 planthopper *Nilaparvata lugens*, has not been reported.
- 41 ● We investigated the density-dependent population dynamics in *N. lugens* by using two
42 populations with high- and low-fecundity genotype.
- 43 ● Under high population densities, the fecundity and population growth rate of the two
44 genotypes of *N. lugens* showed opposite trends across generations.
- 45 ● The key gene *Nlpale* encoding a tyrosine hydroxylase was identified using RNA-seq and
46 bioinformatics analysis.
- 47 ● RNAi study confirmed the dopamine biosynthesis plays a vital role for the two
48 genotypes of *N. lugens* in response to density changes.

49

50 **Introduction**

51 Insects comprise the most diverse class of animals due to their excellent adaptability and high
52 reproductive capacity (Grimaldi and Engel 2005). The reproductive fitness of insects is a
53 quantitative phenotype determined by both of genotypes and the environmental factors.
54 Genotypic factors usually refer to genetic variants that change the function of
55 fecundity-related proteins (Watt 1992; Edward et al. 2014). And environmental factors
56 associated with insect fecundity usually include predators (Rosenheim 1998), temperature
57 (Geister et al. 2008), xenobiotics (Ge et al. 2011), nutrition (Winkler et al. 2006), and the
58 density of insect populations (Stiling 1988). However, how genotypes interact with the
59 environment to modulate the fecundity in a specific insect is largely unknown, due to the lack
60 of appropriate experimental materials.

61 Population density acting as a dynamic factor that closely related to insect diet and the
62 available nutrition, has great impact on the population growth of insects (Hassel 1975; Stiling
63 1988). Population density is critical to the survival and development of the larvae, and
64 consequently impact the fecundity of the emerged adults in a variety of insect species. *Aedes*
65 *aegypti* reared in higher larval density showed a greater number of eggs laid (Silva et al.
66 2020), while *Chilo partellus* moths at lower pairing density had higher fecundity (Hari et al.
67 2008). Increased initial density resulted in prolonged nymphal development duration, lower
68 emergence rate, shorter longevity and lower female fecundity in the rice planthopper (Mori
69 and Nakasuji 1991; Horgan et al. 2016). Besides, population density can influence many other
70 processes, such as predator and prey, parasite and host interactions, disease transmission, and
71 competition (Arcese and Smith 1988; Pacala and Hassell 1991; Berg 1992). Thus, the density
72 stress is an ideal factor to study the interaction between insect genotypes and environment
73 during the regulation of population growth.

74 Previous studies have indicated that population dynamics of insects could be influenced
75 by individual variations (Hanski and Saccheri 2006; Sun et al. 2015). However, it is still a
76 mystery that whether the same population density has equal or diverse impact on insect
77 populations carrying different fitness-determined genotypes. To address this issue, we
78 selected two genotypes of the brown planthopper (BPH), *Nilaparvata lugens*, a serious rice
79 insect pest. Based on our previous studies, we obtained two homozygous BPH populations [a
80 high-fecundity genotype (HFG) and a low-fecundity genotype (LFG) population] from the
81 same initial population, with the ACE₋₈₆₂ and VgR₋₈₁₆ genotypes CCGG and AAAA,
82 respectively (Sun et al. 2015; Liu et al. 2020). In this study, we described the population
83 dynamic of the two genotypes BPH in different initial nymph densities by designing a
84 density-dependent experiment. After that, we applied RNA-seq and a series of bioinformatic
85 analysis to unveil the key factors for density-dependent progenitive phenotypes in this insect.
86 Overall, we aimed to uncover the potential mechanisms behind the insect genotypes and
87 population densities interaction in the modulation of insect fecundity.

88

89 **Materials and methods**

90 **Insect populations and density-dependent bioassays**

91 The BPH populations carrying homozygous high- (HFG) and low-fecundity (LFG) genotypes
92 were previously obtained in our lab (Zhai et al. 2013; Sun et al. 2015), and were reared on a
93 susceptible rice variety (Fenghuazhan) in the greenhouse at 26±2 °C with 70–90% relative
94 humidity and a light-dark cycle of 16L: 8D h.

95 10, 50, 90, 130 and 170 newly (<12 h) hatched nymphs of the two BPH populations were
96 individually reared in the 45-day old rice plants, then the rice plants for each treatment were
97 transferred into a pot covered with insect-proof nets. Ten replicative treatments were
98 conducted for each group. The nymphs' development and survival were recorded daily until
99 becoming adults. The rice plants were replaced timely to keep fresh and sufficient for feeding
100 with each treatment. Two-day-old female adults from each treatment were collected for
101 weighting using electronic balance, then placed immediately in liquid nitrogen and stored at
102 -80°C for subsequent transcriptome sequencing. Those planthoppers in the same density
103 treatment were then mate randomly. When nymphs emerged, we count the number of
104 offsprings from each mate until no nymph hatched for three consecutive days. Those newly
105 emerged nymphs taken from corresponding density treatment were used to conduct the same
106 density-dependent bioassays as the next generation. The density-dependent bioassays were
107 conducted for continuous 6 generations. The population growth rate was calculated as follows:
108 $P = (N * S * R * F * E) / N$ (P: Population growth rate, N: Initial nymph number, S: Nymph survival
109 rate, R: Female ratio, F: Fecundity for per female, E: Egg hatchability) (Yu et al. 2013).

110

111 **RNA extraction and sequencing**

112 The insect samples of HFG and LFG reared under low density (10 nymphs per clump) and
113 high density (170 nymphs per clump) at generations F1, F3 and F5 were collected. Total RNA
114 was subsequently extracted from insect samples with TRIzol Reagent according to the
115 manufacturer's instructions. The RNA samples were utilized for tag library preparation using
116 Illumina gene expression sample preparation kit (Illumina, San Diego, CA, USA), following
117 the manufacturer's instructions. The total RNA integrity and quality were assessed using the
118 RNA 6000 Nano LabChip kit and Agilent 2100 Bioanalyzer (Agilent Technologies, Palo Alto,
119 CA, USA). The poly(A)-containing mRNA was purified using magnetic oligo(dT) beads and
120 the Oligotex mRNA kit (Qiagen, Hilden, Germany). The transcriptome sequencing library

121 was prepared according to a modified method (Su et al. 2012). The mRNA strands were
122 cleaved into short fragments by fragmentation buffer and reverse-transcribed for cDNA
123 synthesis.

124 Two replicates of each treatment were used for RNA sequencing. The cDNA library
125 (~300 base pairs-long) was sequenced using Illumina HiSeq™ 4000 sequencing platform
126 (Illumina, San Diego, CA, USA). The adapter sequences, empty reads, and low-quality
127 sequences (i.e. reads with a ratio of unknown sequences ‘N’ > 5%) were removed to obtain
128 clean reads. All clean reads were mapped to the *N. lugens* genome (Accession No.
129 GCF_000757685.1) with Hisat2 software (Kim et al. 2015). Read counts for all transcripts
130 were extracted with HTSeq-count (Anders et al. 2015) and then transfer to FPKM (Fragments
131 Per Kilobase Million) with R software GenomicFeatures
132 (<https://git.bioconductor.org/packages/GenomicFeatures>).

133

134 **Temporal analysis**

135 We generated a FPKM matrix of all transcripts in all samples. Then the samples were divided
136 into four groups: HFG under low density (HFG-LD), HFG under high density (HFG-HD),
137 LFG under low density (LFG-LD), and LFG under high density (HFG-HD). For each group,
138 the temporal expression pattern from F1 to F5 of all genes was calculated with the
139 corresponding FPKM matrix by using the Short Time-series Expression Miner (STEM)
140 software (Ernst and Bar-Joseph 2006). The cluster number was set to 12 for each analysis.

141

142 **Identification and annotation of candidate co-expression gene modules**

143 Genes with FPKM lower than 0.3 in a sample were considered as “too lowly expressed”
144 (Kang et al. 2013; Bai et al. 2015). We filtered the FPKM matrix by removing the transcripts
145 that showed too low expression in more than half of the tested samples. The filtered matrix
146 was then used for inferring the co-expression gene network modules by using weighted gene
147 co-expression network analysis (WGCNA) in R (Langfelder and Horvath 2008). The
148 parameters were set as “power $\beta = 6$, min module size = 50, ME miss thread = 0.25”.

149 The candidate co-expression gene modules were selected according to the temporally
150 analyzed gene list. The genes in candidate modules were annotated to the KEGG pathway

151 database, and the pathway enrichment analysis was performed based on the Fisher's exact test
152 with Benjamini and Hochberg (BH) adjustment by using the KEGG annotation of all genes in
153 the BPH as background.

154

155 **Differential expression analysis and quantitative real-time PCR validation**

156 The read counts generated by HTseq-count were normalized using R package DESeq2 (Love
157 et al. 2014). Then the differentially expressed genes (DEGs) between pairwise comparisons
158 were estimated by DESeq2 according to the threshold of $|\log_2 \text{ratio}| > 1$ and adjusted P -value
159 < 0.05 (BH adjustment).

160 To support the analysis, twenty DEGs were randomly selected for measurement of
161 expression. Total RNA (1 μg) reverse-transcribed into first-strand cDNA using a PrimeScript™
162 RT reagent kit (Takara Bio, Inc. Otsu, Shiga, Japan). qPCR was performed using a 10- μL
163 reaction containing 1 μL cDNA, 0.3 μL each of 10 $\mu\text{mol}\cdot\text{L}^{-1}$ forward and reverse primers, and
164 5 μL SYBR® FAST Universal qPCR mix (KAPA Biosystems, Woburn, MA, USA) and
165 LightCycler 480 system (Roche Diagnostics GmbH, Mannheim, Germany), with the
166 following amplification conditions: 5 min at 95°C, followed by 45 cycles at 95°C for 10 s, at
167 60°C for 20 s, and at 72°C for 20 s. The qPCR experiments were performed for each sample
168 using three biological and three technical replicates. The expression levels of selected genes
169 were normalized to the expression levels of *N. lugens* β -actin (Chen et al. 2013). The
170 differential gene expression was calculated using the $2^{-\Delta\Delta\text{Ct}}$ method (Livak and Schmittgen,
171 2001).

172

173 **RNA interference of *Nlpale***

174 Gene *Nlpale* encoding tyrosine hydroxylase [(TH; the rate-limiting enzyme in dopamine
175 production metabolic pathway] was selected as the key regulatory factor, and its function was
176 validated by RNA interference (RNAi). For double-stranded RNA (dsRNA) synthesis, a
177 466-bp fragment (*Nlpale*) were amplified by PCR using *Nlpale* cDNAs. All primers contained
178 the T7 promoter sequence at each end (Table S1). The dsRNA of *Aequorea victoria* green
179 fluorescent protein (GFP, Accession No. ACY56286) was used as a control (Qiu et al. 2016;
180 Pang et al. 2017). The T7 RiboMAX Express RNAi System (Promega, USA) was used to

181 synthesize dsRNA according to the manufacturer's instructions. The concentrations of dsRNA
182 were quantified spectrophotometrically with a NanoDrop 2000 instrument (Thermo Fisher
183 Scientific, Waltham, MA, USA). Finally, the quality and size of the dsRNA were further
184 verified via 1% agarose gel electrophoresis.

185 The 1-day-old female adults of HFG and LFG were used for RNAi. The dsRNA injection
186 experiment was mainly conducted as previously described (Chen et al. 2013). Briefly,
187 approximately 250 ng dsRNA was injected into the mesothorax of the individuals. Three
188 females were randomly collected to test the RNAi efficiency by quantitative real-time PCR
189 (qRT-PCR) at 24 h after injection. Then the injected females were mated with male adults at
190 the ratio 1:1, and were released to potted rice according to the densities of 10, 90, and 170
191 individuals respectively. The method for qRT-PCR and fecundity bioassay of the treated
192 insects was as described above. The total number of offsprings from each treatment was
193 counted.

194

195 **Manipulation of dopamine in the BPH**

196 The Insect Dopamine elisa kit (Boshen Biotechnology, Jiangsu, China) was applied to detect
197 the dopamine content in the BPH following the manufacturer's instruction. In brief, every five
198 1-day-old female adults was used as one repeat and six repeats was conducted for each
199 treatment. The homogenate, standard substance and horse radish peroxidase (HRP) labeled
200 antibody of dopamine were successively added to the micropores that are precoated with the
201 dopamine antibody, and were incubated in 37°C. Then the incubation was washed, and the
202 substrate 3', 3', 5', 5', -tetramethyl benzidine (TMB) is used for color rendering. The
203 absorbance (OD value) was measured at the wavelength of 450 nm to reflect the dopamine
204 content in the samples.

205 Dopamine hydrochloride (Sigma-Aldrich), a dopamine activator, and chlorpromazine
206 (CPZ), which was a dopamine receptor antagonist, were dissolved in ringer's solution. The
207 pharmacological injection experiment was mainly conducted as previously described (Ma et
208 al. 2011; Chen et al. 2013). The injection metering of dopamine hydrochloride is 100 nl of
209 80µg/µl while CPZ is 100 nl of 20µg/µl solution. They were injected into the mesothorax of
210 the BPH. Ringer's solution was used as the control. The qRT-PCR and fecundity bioassay

211 after injection was the same as described above.

212

213 **Detection of the hormone 20 - hydroxyecdysone content**

214 The content of hormone 20 - hydroxyecdysone (20E) in the BPH was detected with the Insect
215 Ecdysone ELISA Assay kit (Boshen Biotechnology) according to the manufacturer's
216 instruction. Briefly, every five 1-day-old female adults was used as one repeat and six repeats
217 was conducted for each treatment. The homogenate, standard substance and
218 horse radish peroxidase (HRP) labeled antibody of ecdysone were successively added to the
219 micropores that are precoated with the ecdysone antibody, and were incubated in 37°C. Then
220 the incubation was washed, and the substrate 3', 3', 5', 5', -tetramethyl benzidine (TMB) is
221 used for color rendering. The absorbance (OD value) was measured at the wavelength of 450
222 nm to reflect the ecdysone content in the samples.

223

224 **Statistical analysis**

225 The impact of density, generation, genotype and their combinations on insect fecundity and
226 population growth rate was analyzed with multi-factor analysis of variance (multi-way
227 ANOVA) and Tukey's test using SPSS 18.0 statistical software. The differences in pairwise
228 comparison on gene expression levels and offspring number of the BPH were analyzed with
229 student's *t*-test using SPSS 18.0. Statistical differences were considered significant at $P < 0.05$
230 or very significant at $P < 0.01$. The differences amongst multiple comparisons were tested by
231 one-way ANOVA, followed by Duncan's least significant ranges (LSR) test for multiple
232 comparisons ($P < 0.05$).

233

234 **Results**

235 **Population density modulates the fecundity of BPH**

236 The population growth trends and dynamics between HFG and LFG under the densities of 10,
237 50, 90, 130 and 170 nymphs were measured for 6 continuous generations. The density,
238 generation, genotype and the combinations of these factors all had significant impacts on the
239 number of offspring per female (Table S2). Both genotypes showed a lower fecundity in a
240 higher individual density (Fig. 1A). Under the densities of 90, 130 and 170 nymphs, the

241 offspring number of HFG showed a decreased trend across generations, while the tendencies
242 under low densities (10 and 50 nymphs) were opposite. In contrast, the LFG showed higher
243 fecundity as the generation increasing in all tested densities except for the highest one (170
244 nymphs). There was no significant difference between most adjacent generations in LFG
245 under the density of 170 nymphs.

246 The differential response to the population density between these two genotypes of BPH
247 was also seen from statistics of the population growth rate (Table S2). The population growth
248 rate of HFG presented a significantly rising trend under low population densities (10 and 50
249 nymphs) and a significantly decreasing trend under high population densities (90, 130 and
250 170 nymphs) (Fig. 1B). The LFG demonstrated similar change in the population growth rate
251 under low densities, however, the changing of the population growth rate was not obvious for
252 LFG under high densities (Fig. 1B). These findings suggested that BPH populations with
253 different fecundity-determined genotypes were quite different in their strategies of population
254 regulation to density changes.

255

256 **Temporal expression trends revealed by RNA-seq**

257 RNA-seq experiments were conducted to explore the key factors responsible for different
258 response to density changes between HFP and LFP. Insects reared on the densities of 10 (low
259 density, LD) and 170 (high density, HD) nymphs were selected, and samples were collected at
260 F1, F3 and F5. The RNA-seq produced an average 33,320,239 clean paired-end reads per
261 sample with Q30 value higher than 92% (Table S3). The average mapping rate of all samples
262 to the reference genome of the BPH was 54.43% (Table S3), and a FPKM matrix of 24,306
263 transcripts in all samples was generated based on the mapping results (Table S4). After
264 filtering the “too lowly expressed” transcripts, 15,147 transcripts were used for subsequent
265 analysis.

266 We applied temporal analysis with the filtered FPKM matrix to each treatment (HFG-LD,
267 HFG-HD, LFG-LD, and LFG-HD) independently. According to the fecundity phenotype, the
268 key factors in both HFG and LFG should show a linear correlation to the fecundity under low
269 density, thus the transcripts showing continuous increasing or decreasing trend along with
270 generations in group HFG-LD and LFG-LD were selected (Fig. 2A). For both genotypes

271 under high density, the key factors should show differential expression patterns to those under
272 low density. Additionally, the expression patterns of key factors between HFG and LFG under
273 high density should also be inconsistent. By using these considerations as filter parameters,
274 we finally identified 31 candidate genes (Fig. 2B). The expression levels of these genes
275 demonstrated significantly high correlation between HFG-LD and LFG-LD, while most of
276 them only show low correlation in the other comparisons (HFG-LD to HFG-HD, LFG-LD to
277 LFG-HD, and HFG-HD to LFG-HD) (Fig. 2C).

278

279 **Identification of the key regulatory factor for density-dependent progenitive phenotypes**

280 To further determine the key factors for density-dependent progenitive phenotypes, we
281 conducted weighted gene co-expression network analysis (WGCNA). All the filtered
282 transcripts were used for this analysis. The analysis resulted in 16 distinct gene modules (Fig.
283 3A, Table S5). The 31 candidate genes were distributed in eight of the modules. Among them,
284 the turquoise and darkred modules accounted for most of the candidate genes (21/31, Table
285 S6). The KEGG pathway enrichment of the genes in these two modules was analyzed. The
286 genes in turquoise module were significantly enriched in a total of 69 pathways, while the
287 number of enriched pathways for the genes in darkred module was 25 (Table S7). Remarkably,
288 four pathways were identified to be enriched for both modules, which included Endocrine and
289 other factor-regulated calcium reabsorption, Axon regeneration, Dopaminergic synapse, and
290 Regulation of actin cytoskeleton (Fig. 3B). This finding suggested that these pathways might
291 play important roles in regulation of fecundity between different population densities.

292 According to the phenotypic difference, the key factors should show significantly
293 differential expression between HFG-HD and HFG-LD at F5. Thus, a differential expression
294 analysis was conducted on these two datasets. The analysis identified a total of 464 DEGs in
295 HFG-HD compared to HFG-LD, including 311 up-regulated and 153 down-regulated genes
296 (Fig.4A, Table S8). Among the DEGs, only six were involved in the above four pathways.
297 And importantly, only one of the 6 DEGs belonged to the candidate transcripts obtained from
298 the temporal analysis. This candidate gene, LOC111049383 (*Nlpale*), encodes tyrosine
299 hydroxylase that is the key rate-limiting enzyme for dopamine synthesis in organisms
300 (Morgan et al. 1996; Ma et al. 2011) (Fig. 4B). The decreased expression trend of gene *Nlpale*

301 in low population density was irrelevant to the fecundity genotypes of BPH (Fig. 4B).
302 However, the expression level of *Nlpale* was continuously elevated in HFG under high
303 population density with the generations increasing, but similar trend was not seen in LFG
304 under the same treatment. Overall, the expression changes of *pale* were negatively correlated
305 to the phenotypic changes of fecundity in both genotypes of BPH.

306

307 **The modulation of gene *Nlpale* and dopamine in the progenitive plasticity of BPH**

308 The insects of HFG and LFG under low population fecundity (10 nymphs) were used to
309 determine the basic expression level of gene *Nlpale* and content of dopamine in different
310 genotypes of BPH. Based on the qRT-PCR analysis, the mRNA level of *Nlpale* was much
311 higher in LFG than that in HFG (Fig. 5A). Accordingly, the LFG showed higher content of
312 dopamine than the HFG (Fig. 5B). These results were corresponding to the transcriptomic
313 analysis that the expression of gene *Nlpale* and the fecundity of BPH were negative
314 correlation. This negative regulatory relationship was further confirmed by RNAi of *Nlpale*.
315 The expression of *Nlpale* in insects of both genotypes was significantly decreased from 24 to
316 72 h after injection of dsRNA, compared with the GFP control (Fig. 5C). Interestingly, the
317 expression of *NIVg*, an important molecular marker for insect fecundity, were significantly
318 increased in insects of both genotypes at 48 and 72 h after RNAi of *Nlpale* (Fig. 5D).
319 Correspondingly, the offspring number of HFG and LFG was significantly elevated after
320 RNAi of *Nlpale* (Fig. 5E). In addition, when the female adults were supplied with extra
321 dopamine hydrochloride by micro-injection, their offspring number was significantly declined.
322 And the injection of CPZ, a dopamine inhibitor, resulted in the increasing of offspring number
323 in corresponding female adults (Fig. 5F). The negative correlation between dopamine content
324 and fecundity had no difference between insects of HFG and LFG, indicating the intrinsic
325 regulatory role of dopamine biosynthesis in the fecundity of BPH.

326 We further investigated that whether *Nlpale* and dopamine were the key factors to
327 determine the difference in response to population density changes between HFG and LFG
328 insects. A significant correlation between the content of dopamine and the fecundity were
329 observed on the insects from both genotypes under different population densities across 6
330 generations ($R=-0.88$ and $P\text{-value}=1.52\times 10^{-6}$ for HFG, and $R=-0.90$ and $P\text{-value}=3.45\times 10^{-7}$

331 for LFG, Fig. S1). Then the fecundity of *Nlpale* RNAi-treated insects of both genotypes was
332 compared to those of GFP control. In the control traits, the average fecundity of both
333 genotypes was significantly decreased as the population density increasing (Fig. 6A). When
334 the *Nlpale* was knockdown, the density-dependent change of fecundity in LFG were almost
335 disappeared (Fig. 6B). However, the absence of density effect only found in the HFG under
336 high population density (130 and 170 nymphs). We subsequently modulated the content of
337 dopamine in the insects of HFG and LFG. Interestingly, the injection of dopamine
338 hydrochloride and CPZ all eliminated the density effect on fecundity of LFG, and similar
339 result was only observed on high population density-treated samples of the HFG (Fig.6C and
340 6D). These results suggested that the disruption of dopamine biosynthesis has great impact on
341 the density-dependent progenitive plasticity of BPH.

342 Previous studies have showed that the dopamine can regulate the biosynthesis of other
343 insect hormones (Gruntenko et al. 2005a; 2005b; Rauschenbach et al. 2007). Thus, the
344 relationship between the hormone 20E and dopamine in this density-dependent experiment
345 was assessed. Accordingly, the content of 20E was negatively correlated to the dopamine
346 content but positively correlated to the fecundity in BPH samples under different densities
347 across different generations (Fig. S1). Additionally, the RNAi of gene *Nlpale* lead to the
348 increase of 20E in the insect of both genotypes (Fig. S2), indicating the intrinsic regulation
349 relationship between dopamine and 20E in this species.

350

351 **Discussion**

352 In the present study, we validated the progenitive plasticity in the BPH populations with two
353 different fecundity-related genotypes. Under the continuous condition of low density, the
354 insect population continuously expanded by the elevation of individual fecundity, and this
355 elevation was independent of the genotypes. When under the continuous high density, the
356 HFG insect continuously reduced its individual fecundity as well as the population growth
357 rate, but this decreasing trend was not observed on the LFG (Fig. 1).

358 Our findings can be largely explained by the traditional theory of density-dependent
359 population regulation. Nicholson (1933) proposed that the population could adjust density
360 according to its own natural and environmental conditions. All species would balance their

361 population density with the resources which they need to live. Accordingly, a population
362 density higher than the balance can be restricted by a series of morphological, physiological,
363 behavioral, and genetic factors to prevent the population from infinite growing (Chitty 1960).
364 In turn, the factors suppressing population growth will be weakened if the population density
365 is lower than the balance (Murdoch 1994; Turchin 1999). The changes in the population
366 growth rate of treatments LFG-LD, HFG-LD and HFG-HD were basically conformed with
367 this hypothesis. For the treatment of LFG under high density, the fecundity showed increased
368 trends but the population growth rate was overall stable across different generations. One
369 possibility was that there exist some thresholds for population balance under different
370 densities in this species. For high density, the threshold was to the advantage of LFG. Thus,
371 the LFG under these densities could rapidly reach the state of balance, as was observed from
372 the stabilized population growth rates.

373 RNA-seq and a series of bioinformatic analysis were utilized to unveil the determinant
374 for the phenotypic difference between HFG and LFG under high population density. The
375 analyzed results centralized at four pathways (Fig. 3B). Interestingly, all these pathways were
376 closely related to the neural system. The Regulation of actin cytoskeleton is an essential
377 process during axonogenesis, because that the neuroblast growth must undergo an
378 engorgement that involves depolymerization of actin (Bradke and Dotti 1999) followed by the
379 penetration of the microtubules into the central and peripheral domains (Kunda et al. 2001).
380 Endocrine and other factor-regulated calcium reabsorption is a pathway associated with
381 calcium regulation in organism, while calcium ion plays an important role in the activity of
382 neural synaptotagmin (Li et al. 1995; Tucker et al. 2004). Importantly, the pathways of Axon
383 regeneration and Dopaminergic synapse were exactly the components of the neural system
384 (Neve et al. 2004; Hammarlund and Jin 2014).

385 Our subsequent research found that the dopamine was the key factor in modulating the
386 fecundity of BPH. Interestingly, it seems that the fecundity was negative correlated to its
387 dopamine content in the BPH (Fig. 4 and Fig. 5). Dopamine is a catecholamine
388 neurotransmitter that is synthesized in both neuronal and non-neuronal tissues. It plays an
389 important role in insect development and is known to be involved in insect's stress responses
390 (Neckameyer 1996; Neckameyer and Weinstein 2005). Dopamine can act as a

391 neuromodulator to stimulate behavior like arousal, reproductive and locomotor activity
392 (Neckameyer et al. 2000; Pendleton et al. 2002; Pfeiffenberger and Allada 2012).
393 Environmental stress, such as heat, parasite infection can affect dopaminergic signaling
394 pathways in insects, then in turn, insects can benefit from dopamine to adapt to external
395 environment by modulating ontogenesis and development (Hirashima et al. 2000; Gruntenko
396 et al. 2000, 2004; Lavista-Llanos et al. 2014). Actually, it has been previously reported that
397 dopamine can also regulate insect reproduction by modulating female sexual receptivity,
398 oogenesis, and oviposition (Neckameyer 1998; Boulay 2001). Meanwhile, the change in
399 dopamine content can cause the changes in other hormones like 20E and JH, indicating its
400 potential regulative role to these hormones (Gruntenko et al. 2005a, 2005b; Rauschenbach et
401 al. 2007). Our data also suggested that the 20E content was negatively regulated by the
402 dopamine (Fig. S2). In BPH, the 20E content in female adults is significant associated with
403 their progenitive capacity (Yu et al. 2014; Zhou et al. 2020). Thus, the regulation of dopamine
404 biosynthesis on the fecundity of BPH may go through the 20E signal pathway. Further
405 research will be conducted to investigate this regulative approach.

406 More importantly, our study showed that dopamine exactly contributed to the
407 density-dependent progenitive plasticity of BPH. Both RNAi of the tyrosine hydroxylase
408 coding gene (*Nlpale*) and modulating of the dopamine content in insects significantly
409 disturbed the density effect on the fecundity of BPH (Fig. 6). In *Locusta migratoria*, the
410 transitions between solitary and gregarious phases in response to population density changes
411 are closely related to dopamine biosynthesis (Ma et al. 2011; Zhang et al. 2020). Here, we
412 assumed that the different population densities would release different signals to the brain of
413 insects, which differentially regulate the pathway of dopamine synthesis and thus result in the
414 different changes in female fecundity. The trend of phenotypic change across generations is
415 finally determined by the population genotype that is associated to the distance to population
416 balance under a specific density.

417 In summary, we demonstrated that the dopamine biosynthesis is the key regulatory factor
418 for density-dependent progenitive plasticity in the BPH. The findings in this study provide
419 insights into the interaction of genotypes and environmental factors in regulating insect
420 population dynamics, and will facilitate the understanding of the mechanism behind the

421 population regulation.

422

423 **Acknowledgements**

424 This work was supported by the National Natural Science Foundation of China (31672021
425 and 31730073), and the Young Innovative Talents Project of Ordinary University of
426 Guangdong Province, China (KA2001961).

427

428 **Data Accessibility**

429 All sequencing data were deposited to the NCBI Sequence Read Archive (SRA;
430 <http://www.ncbi.nlm.nih.gov/sra/>) under the BioProject PRJNA690237.

431

432 **Author Contributions**

433 KL, WZ and RP conceived and designed the study. KL, RP, WC and KK conduct the
434 experiments. KL and RP designed the RNA-seq analysis pipeline, and performed the data
435 analysis. LYY, LY, and JL contributed to materials. KL, WZ and RP wrote the manuscript.

436

437 **References**

438 Anders S, Pyl PT, Huber W (2015) HTSeq-a Python framework to work with high-throughput
439 sequencing data. *Bioinformatics* 31:166-169.

440 <https://doi.org/10.1093/bioinformatics/btu638>

441 Arcese P, Smith JNM (1988) Effects of population-density and supplemental food on
442 reproduction in song sparrows. *J Anim Ecol* 57:119-136. <https://doi.org/10.2307/4768>

443 Bai Y, Dougherty L, Cheng LL, Zhong GY, Xu KN (2015) Uncovering co-expression gene
444 network modules regulating fruit acidity in diverse apples. *BMC Genomics* 16:612.

445 <https://doi.org/10.1186/s12864-015-1816-6>

446 Bainton RJ, Tsai LT, Singh CM, Moore MS, Neckameyer WS, Heberlein U (2000) Dopamine
447 modulates acute responses to cocaine, nicotine and ethanol in *Drosophila*. *Curr Biol*
448 10:187-194. [https://doi.org/10.1016/s0960-9822\(00\)00336-5](https://doi.org/10.1016/s0960-9822(00)00336-5)

449 Berg A, Lindberg T, Kallebrink KG (1992) Hatching success of lapwings on farmland
450 differences between habitats and colonies of different sizes. *J Anim Ecol* 61:469-476.

451 <https://doi.org/10.2307/5337>

452 Boulay R, Hooper-Bui LM, Woodring J (2001) Oviposition and oogenesis in virgin fire ant
453 females *Solenopsis invicta* are associated with a high level of dopamine in the brain.
454 *Physiol Entomol* 26:294-299. <https://doi.org/10.1046/j.0307-6962.2001.00250.x>

455 Bradke F, Dotti CG (1999) The role of local actin instability in axon formation. *Science*
456 283:1931-1934. <https://doi.org/10.1126/science.283.5409.1931>

457 Chen J, Liang Z, Liang Y, Pang R, Zhang W (2013) Conserved microRNAs miR-8-5p and
458 miR-2a-3p modulate chitin biosynthesis in response to 20-hydroxyecdysone signaling in
459 the brown planthopper, *Nilaparvata lugens*. *Insect Biochem Molec* 43:839-848.
460 <https://doi.org/>

461 Chitty D (1960) Population processes in the vole and their relevance to general theory. *Can J*
462 *Zool* 38: 99-113. <https://doi.org/10.1139/z60-011>

463 Edward DA, Poissant J, Wilson AJ, Chapman T (2014) Sexual conflict and interacting
464 phenotypes: a quantitative genetic analysis of fecundity and copula duration in
465 *Drosophila Melanogaster*. *Evolution*, 68:1651-1660. <https://doi.org/10.1111/evo.12376>

466 Ernst J, Bar-Joseph Z (2006) STEM: a tool for the analysis of short time series gene
467 expression data. *BMC Bioinformatics* 7:191. <https://doi.org/10.1186/1471-2105-7-191>

468 Ge LQ, Cheng Y, Wu JC, Jahn GC (2011) Proteomic analysis of insecticide
469 triazophos-induced mating-responsive proteins of *Nilaparvata lugens* Stål (Hemiptera:
470 Delphacidae). *J Proteome Res* 10:4597-4612. <https://doi.org/10.1021/pr200414g>

471 Geister TL, Lorenz MW, Meyering-Vos M, Hoffmann KH, Fischer K (2008) Effects of
472 temperature on reproductive output, egg provisioning, juvenile hormone and vitellogenin
473 titres in the butterfly *Bicyclus anynana*. *J Insect Physiol* 54:1253-1260.
474 <https://doi.org/10.1016/j.jinsphys.2008.06.002>

475 Grimaldi D, Engel MS (2005) Evolution of the insects. Cambridge University Press,
476 Cambridge, New York

477 Gruntenko NE, Karpova EK, Adonyeva NV, Chentsova NA, Faddeeva NV, Alekseev AA,
478 Rauschenbach IY (2005a) Juvenile hormone, 20-hydroxyecdysone and dopamine
479 interaction in *Drosophila virilis* reproduction under normal and nutritional stress
480 conditions. *J Insect Physiol* 51:417-425. <https://doi.org/10.1016/j.jinsphys.2005.01.007>

481 Gruntenko NE, Karpova EK, Alekseev AA, Chentsova NA, Saprykina ZV, Bownes M,
482 Rauschenbach IY (2005b) Effects of dopamine on juvenile hormone metabolism and
483 fitness in *Drosophila virilis*. J Insect Physiol 51:959-968.
484 <https://doi.org/10.1016/j.jinsphys.2005.04.010>

485 Gruntenko NE, Khlebodarova TM, Vasenkova IA, Sukhanova MJ, Wilson TG, Rauschenbach
486 IY (2000) Stress-reactivity of a *Drosophila melanogaster* strain with impaired juvenile
487 hormone action. J Insect Physiol 46:451-456.
488 [https://doi.org/10.1016/s0022-1910\(99\)00131-6](https://doi.org/10.1016/s0022-1910(99)00131-6)

489 Gruntenko NE, Raushenbakh IY (2004) Adaptive value of genes controlling the level of
490 biogenic amines in *Drosophila*. Genetika 40:869-876.
491 <https://doi.org/10.1023/B:RUGE.0000036517.62459.8d>

492 Hammarlund M, Jin Y (2014) Axon regeneration in *C. elegans*. Curr Opin Neurobiol
493 27:199-207. <https://doi.org/10.1016/j.conb.2014.04.001>

494 Hanski I, Saccheri I (2006) Molecular-level variation affects population growth in a butterfly
495 metapopulation. PloS Biology 4:719-726. <https://doi.org/10.1371/journal.pbio.0040129>

496 Hari NS, Jindal J, Malhi NS, Khosa JK (2008) Effect of adult nutrition and insect density on
497 the performance of spotted stem borer, *Chilo partellus* in laboratory cultures. J Pest Sci
498 81:23-27. <https://doi.org/10.1007/s10340-007-0180-y>

499 Hassell MP (1975) Density-dependence in single-species populations. J Anim Ecol
500 44:283-295. <https://doi.org/10.2307/3863>

501 Hirashima A, Sukhanova M, Rauschenbach I (2000) Biogenic amines in *Drosophila virilis*
502 under stress conditions. Biosci Biotech Bioch 64:2625-2630. <https://doi.org/10.1080/10808867>

503 Horgan FG, Naik BS, Iswanto EH, Almazan MLP, Ramal AF, Bernal CC (2016) Responses
504 by the brown planthopper, *Nilaparvata lugens*, to conspecific density on resistant and
505 susceptible rice varieties. Entomol Exp Appl 158:284-294.
506 <https://doi.org/10.1111/eea.12400>

507 Kang CY, Darwish O, Geretz A, Shahan R, Alkharouf N, Liu ZC (2013) Genome-scale
508 transcriptomic insights into early-stage fruit development in woodland strawberry
509 *Fragaria vesca*. Plant Cell 25:1960-1978. <https://doi.org/10.1105/tpc.113.111732>

510 Kim D, Landmead B, Salzberg SL (2015) HISAT: a fast spliced aligner with low memory

511 requirements. *Nat Methods* 12:357-360. <https://doi.org/10.1038/nmeth.3317>

512 Kunda P, Paglini G, Quiroga S, Kosik K, Caceres A (2001) Evidence for the involvement of
513 Tiam1 in axon formation. *J NEUROSCI* 21:2361-2372.
514 <https://doi.org/10.1523/jneurosci.21-07-02361.2001>

515 Langfelder P, Horvath S (2008) WGCNA: an R package for weighted correlation network
516 analysis. *BMC Bioinformatics* 9:1-32. <https://doi.org/10.1186/1471-2105-9-559>

517 Lavista-Llanos S, Svatos A, Kai M, Thomas R, Serge B, Stensmyr MC, Hansson BS (2014)
518 Dopamine drives *Drosophila sechellia* adaptation to its toxic host. *Elife* 3:e03785.
519 <https://doi.org/10.7554/eLife.03785>

520 Li C, Ullrich B, Zhang JZ, Anderson RGW, Brose N, Südhof TC (1995) Ca²⁺-dependent and
521 -independent activities of neural and non-neural synaptotagmins. *Nature* 375:594-599.
522 <https://doi.org/10.1038/375594a0>

523 Liu K, Chen Z, Su Q, Yue L, Chen WW, Zhang WQ (2020) Comparative analysis of the
524 ecological fitness and transcriptome between two genotypes of the brown planthopper
525 *Nilaparvata lugens*. *J Integr Agr* 19:1501-1511.
526 [https://doi.org/10.1016/S2095-3119\(19\)62768-1](https://doi.org/10.1016/S2095-3119(19)62768-1)

527 Livak KJ, Schmittgen TD (2001) Analysis of relative gene expression data using real-time
528 quantitative PCR and the 2^{-ΔΔCT} method. *Methods* 25:402-408.
529 <https://doi.org/10.1006/meth.2001>

530 Love MI, Huber W, Anders S (2014) Moderated estimation of fold change and dispersion for
531 RNA-seq data with DESeq2. *Genome Biol* 15:31-46.
532 <https://doi.org/10.1186/s13059-014-0550-8>

533 Ma ZY, Guo W, Guo XJ, Wang XH, Kang L (2011) Modulation of behavioral phase changes
534 of the migratory locust by the catecholamine metabolic pathway. *P Natl Acad Sci USA*
535 108:3882-3887. <https://doi.org/10.1073/pnas.1015098108>

536 Morgan WW, Walter CA, Windle JJ, Sharp ZD (1996) 3.6 kb of the 5' flanking DNA activates
537 the mouse tyrosine hydroxylase gene promoter without catecholaminergic-specific
538 expression. *J Neurochem* 66:20-25.
539 <https://doi.org/10.1046/j.1471-4159.1996.66010020.x>

540 Mori K, Nakasuji F (1991) Effects of day length and density on development and wing form

541 of the small brown planthopper, *Laodelphax striatellus* (Hemiptera: Delphacidae). Appl
542 Entomol Zool 26:557-561. <https://doi.org/10.1303/aez.26.557>

543 Murdoch WW (1994) Population regulation in theory and practice. Ecology 75:271-287.
544 <https://doi.org/10.2307/1939533>

545 Neckameyer WS (1996) Multiple roles for dopamine in *Drosophila* development. Dev Biol
546 176:209-219. <https://doi.org/10.1006/dbio.1996.0128>

547 Neckameyer WS (1998) Dopamine modulates female sexual receptivity in *Drosophila*
548 *melanogaster*. J Neurogenet 12:101-114. <https://doi.org/10.3109/01677069809167259>

549 Neckameyer WS, Weinstein JS (2005) Stress affects dopaminergic signaling pathways in
550 *Drosophila melanogaster*. Stress 8:117-131.
551 <https://doi.org/10.1080/10253890500147381>

552 Neve KA, Seamans JK, Trantham-Davidson H (2004) Dopamine receptor signaling. J Recept
553 Sig Transd 24:165-205. <https://doi.org/10.1081/RRS-200029981>

554 Nicholson AJ (1933) The balance of animal populations. J Anim Ecol 2:132-178.
555 <https://doi.org/10.2307/954>

556 Pacala SW, Hassell MP (1991) The persistence of host-parasitoid associations in patchy
557 environments. II. evaluation of field data. Am Nat 138:584-605. <https://doi.org/10.2307/2462455>

558

559 Pang R, Qiu JQ, Li TC, Yang P, Yue L, Pan XY, Zhang WQ (2017) The regulation of lipid
560 metabolism by a hypothetical P-loop NTPase and its impact on fecundity of the brown
561 planthopper. BBA-Gen Subjects 1861:1750-1758.
562 <https://doi.org/10.1016/j.bbagen.2017.03.011>

563 Pendleton RG, Rasheed A, Sardina T, Tully T, Hillman R (2002) Effects of tyrosine
564 hydroxylase mutants on locomotor activity in *Drosophila*: a study in functional
565 genomics. Behav Genet 32:89-94. <https://doi.org/10.1023/A:1015279221600>

566 Pfeiffenberger C, Allada R (2012) Cul3 and the BTB adaptor insomniac are key regulators of
567 sleep homeostasis and a dopamine arousal pathway in *Drosophila*. PLoS Genet
568 8:e1003003. <https://doi.org/10.1371/journal.pgen.1003003>

569 Qiu J, He Y, Zhang J, Kang K, Li T, Zhang WQ (2016) Discovery and functional
570 identification of fecundity-related genes in the brown planthopper by large-scale RNA

571 interference. *Insect Mol Biol* 25:724-733. <https://doi.org/10.1111/imb.12257>

572 Rauschenbach IY, Chentsova NA, Alekseev AA, Gruntenko NE, Adonyeva NV, Karpova EK,
573 Bowens M (2007) Dopamine and octopamine regulate 20-hydroxyecdysone level in vivo
574 in *Drosophila*. *Arch Insect Biochem* 65:95-102. <https://doi.org/10.1002/arch.20183>

575 Rosenheim JA (1998) Higher-order predators and the regulation of insect herbivore
576 populations. *Annu Rev Entomol* 43:421-447.
577 <https://doi.org/10.1146/annurev.ento.43.1.421>

578 Silva RM, Santos LV, Caiado MS, Hastenreiter SN (2020) The influence of larval density on
579 triacylglycerol content in *Aedes aegypti* (Linnaeus) (Diptera: Culicidae). *Arch Insect*
580 *Biochem* e21757. <https://doi.org/10.1002/arch.21757>

581 Stiling P (1988) Density-dependent processes and key factors in insect populations. *J Anim*
582 *Ecol* 57:581-593. <https://doi.org/10.2307/4926>

583 Sun ZX, Zhai YF, Zhang JQ, Kang K, Cai JH, Fu YG, Zhang WQ (2015) The genetic basis of
584 population fecundity prediction across multiple field populations of *Nilaparvata lugens*.
585 *Mol Ecol* 24:771-784. <https://doi.org/10.1111/mec.13069>

586 Tucker WC, Weber T, Chapman ER (2004) Reconstitution of Ca²⁺-regulated membrane fusion
587 by synaptotagmin and SNAREs. *Science* 304:435-438.
588 <https://doi.org/10.1126/science.1097196>

589 Turchin P (1999) Population regulation: a synthetic view. *Oikos* 84:153-159.
590 <https://doi.org/10.1353/pbm.2012.0039>

591 Watt WB (1992) Eggs, enzymes, and evolution: natural genetic variants change insect
592 fecundity. *P Natl Acad Sci USA* 89:10608-10612.
593 <https://doi.org/10.1073/pnas.89.22.10608>

594 Winkler K, Wackers F, Bukovinszkine-Kiss G, van Lenteren J (2006) Sugar resources are
595 vital for *Diadegma semiclausum* fecundity under field conditions. *Basic Appl Ecol*
596 7:133-140. <https://doi.org/10.1016/j.baae.2005.06.001>

597 Yu R, Xu XP, Liang YK, Tian HG, Pan ZQ, Jin SH, Zhang WQ (2014) The insect ecdysone
598 receptor is a good potential target for RNAi-based pest control. *Int J Biol Sci*
599 10:1171-1180. <https://doi.org/10.7150/ijbs.9598>

600 Yu Y, Xu HX, Zheng XS, Yang YJ, Lu ZX (2013) Effects of drought stress on the ecological

601 fitness of brown planthopper, *Nilaparvata lugens* at high temperature. Acta Phytophy Sin,
602 40:193-199. <https://doi.org/10.13802/j.cnki.zwbhxb.2013.03.001>
603 Zhai YF, Zhang JQ, Sun ZX, Dong XL, He Y, Kang K, Zhang, WQ (2013) Proteomic and
604 transcriptomic analyses of fecundity in the brown planthopper *Nilaparvata lugens* (Stål).
605 J Proteome Res 12:5199-5212. <https://doi.org/10.1021/pr400561c>
606 Zhang X, Xu YN, Chen B, Kang L (2020) Long noncoding RNA PAHAL modulates locust
607 behavioural plasticity through the feedback regulation of dopamine biosynthesis. Plos
608 Genet 16:e1008771. <https://doi.org/10.1371/journal.pgen.1008771>
609 Zhou X, Ye YZ, Ogihara MH, Takeshima M, Fujinaga D, Liu CW, Bao YY (2020) Functional
610 analysis of ecdysteroid biosynthetic enzymes of the rice planthopper, *Nilaparvata lugens*.
611 Insect Biochem Molec 123:103428. <https://doi.org/10.1016/j.ibmb.2020.103428>

612

613 **Figure legends**

614 **Fig. 1** The influence of population density on the fecundity (**a**) and population growth rate (**b**)
615 of two BPH populations with different fecundity-related genotypes. HFG: High-fecundity
616 genotype BPH; LFG: Low-fecundity genotype BPH. **a** F1-F6 represent the 1st to 6th
617 generation of nymph density experiment, respectively. The values are presented as mean \pm SE
618 ($n=10$). The values sharing different lowercase letters are significantly different at $P < 0.05$
619 (one-way ANOVA and Duncan's multiple range test).

620

621 **Fig. 2** Temporal expression trend analysis of the transcriptome data. **a** Clusters of gene
622 expression trends by the Short Time-series Expression Miner (STEM) software. The gene
623 clusters 1 and 10 of treatments HFG-LD and LFG-LD were selected. **b** Heatmap representing
624 the expression patterns of 31 candidate genes in each treatment. The trends indicate the
625 expression patterns in treatments HFG-LD and LFG-LD. **c** The Pearson correlation
626 coefficient of pairwise comparison on the expression levels of candidate genes.

627

628 **Fig. 3** Identification of co-expression genes related to candidate genes by Weighted gene
629 co-expression network analysis (WGCNA). **a** Hierarchical cluster tree showing the
630 co-expression modules identified by WGCNA. **b** The overlapped pathways that are enriched

631 for gene modules turquoise and darkred.

632

633 **Fig. 4** Targeting the key regulatory factors by differential expression analysis. **a** A volcano
634 plot of the gene expression pattern between HFG-HD and HFG-LD at F5. The black, red and
635 green points represent no difference in expression, up-regulated genes and down-regulated
636 genes ($FDR \leq 0.05$, Benjamini and Hochberg adjustment). **b** The pathway map of
637 Dopaminergic synapse. The expression patterns of detected genes in this pathway are
638 presented by heatmap.

639

640 **Fig.5** The role of *Nlpale* mRNA level and dopamine content in the fecundity of BPH. The
641 *Nlpale* mRNA levels (**a**) and dopamine contents (**b**) in two genotypes insects are presented.
642 The mRNA levels of *Nlpale* (**c**) and *NIVg* (**d**) in the two genotypes of BPH were measured at
643 24, 48 and 72 h after RNA interference of *Nlpale*. The insects injected with *dsGFP* were used
644 as control. **e** The fecundity of HFG and LFG after injection of *Nlpale* dsRNA. **f** The fecundity
645 of HFG and LFG after injection of dopamine inhibitor chlorpromazine, dopamine
646 hydrochloride (activator), and water control. All data are presented as mean \pm SE. *: $P < 0.05$
647 level; **: $P < 0.01$ level (student's *t*-test). The values sharing different letters are significantly
648 different at $P < 0.05$ (one-way ANOVA and Duncan's multiple range test).

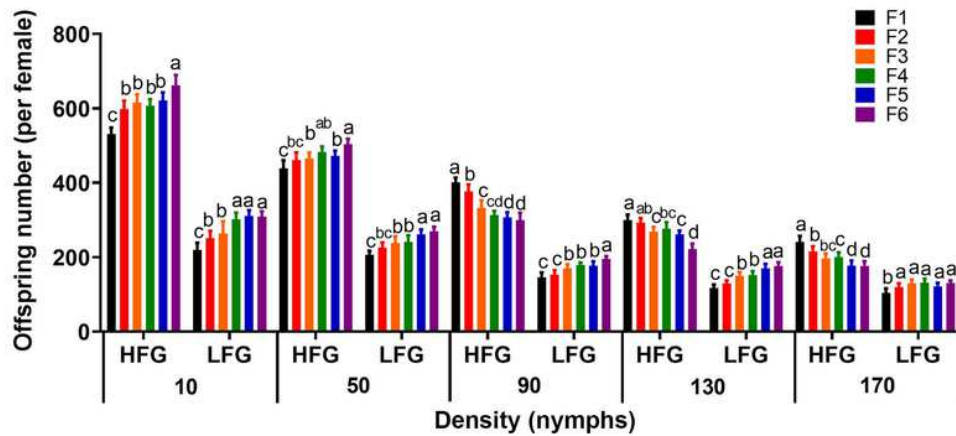
649

650 **Fig. 6** The role of dopamine biosynthesis in the density-dependent effects on the fecundity of
651 BPH. The impact of injection of *dsGFP* (**a**), *dsNlpale* (**b**), dopamine hydrochloride (**c**), and
652 chlorpromazine (**d**) on the fecundity of two genotypes insects under the population densities
653 of 10, 50, 90, 130 and 170 individuals. All data are presented as mean \pm SE. The values
654 sharing different capital letters are significantly different at $P < 0.05$ within the HFG, and the
655 values sharing different lowercase letter are significantly different at $P < 0.05$ within the LFG
656 (one-way ANOVA and Duncan's multiple range test).

657

Figures

a



b

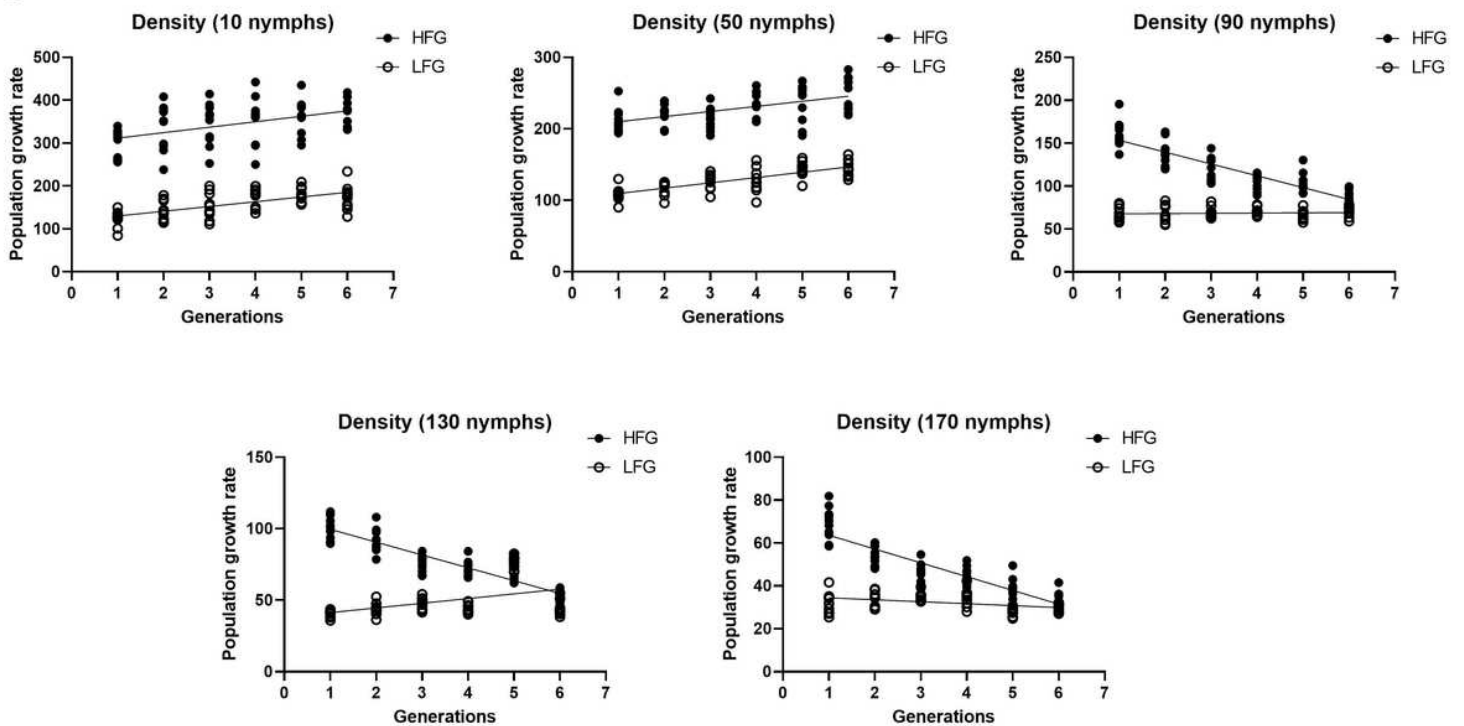


Figure 1

The influence of population density on the fecundity (a) and population growth rate (b) of two BPH populations with different fecundity related genotypes. HFG: High fecundity genotype BPH; LFG: Low fecundity genotype BPH. a F1 F6 represent the 1st to 6th generation of nymph density experiment, respectively. The values are presented as mean \pm SE (n=10). The values sharing different lowercase letters are significantly different at P < 0.05 (one way ANOVA and Duncan's multiple range test).

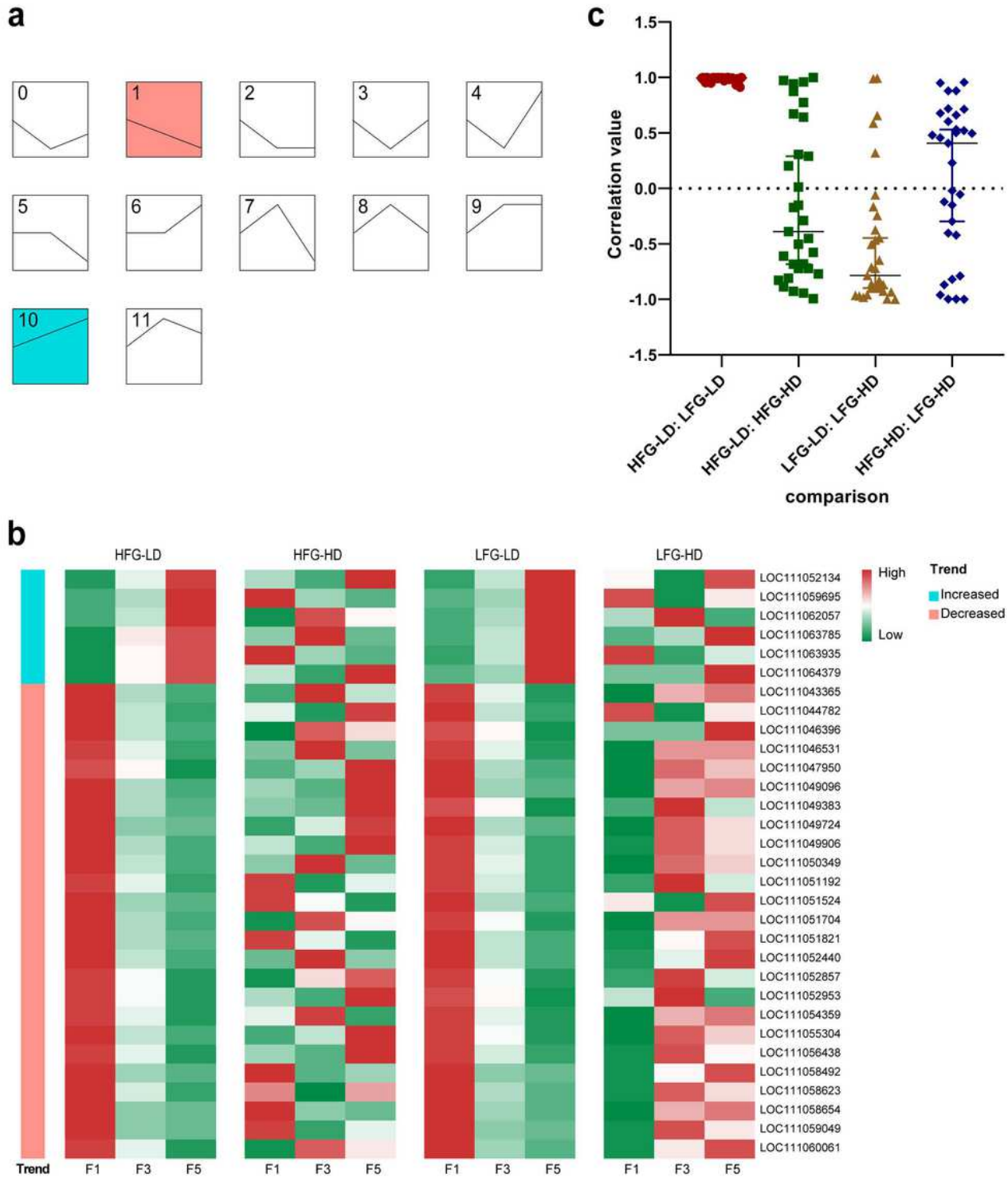


Figure 2

Temporal expression trend analysis of the transcriptome data. a Clusters of gene expression trends by the Short Time series Expression Miner (STEM) software. The gene clusters 1 and 10 of treatments HFG LD and LFG LD were selected. b Heatmap representing the expression patterns of 31 candidate genes in each treatment. The trends indicate the expression patterns in treatments HFG LD and LFG LD. c The Pearson correlation coefficient of pairwise comparison on the expression levels of candidate genes.

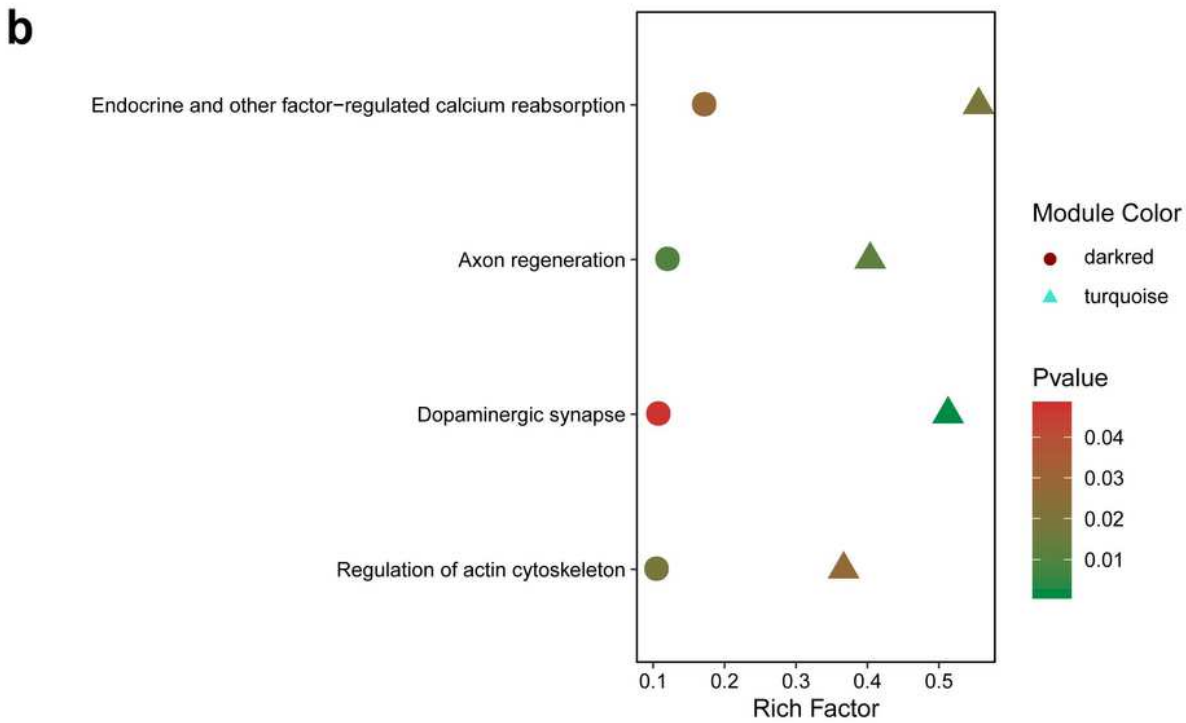
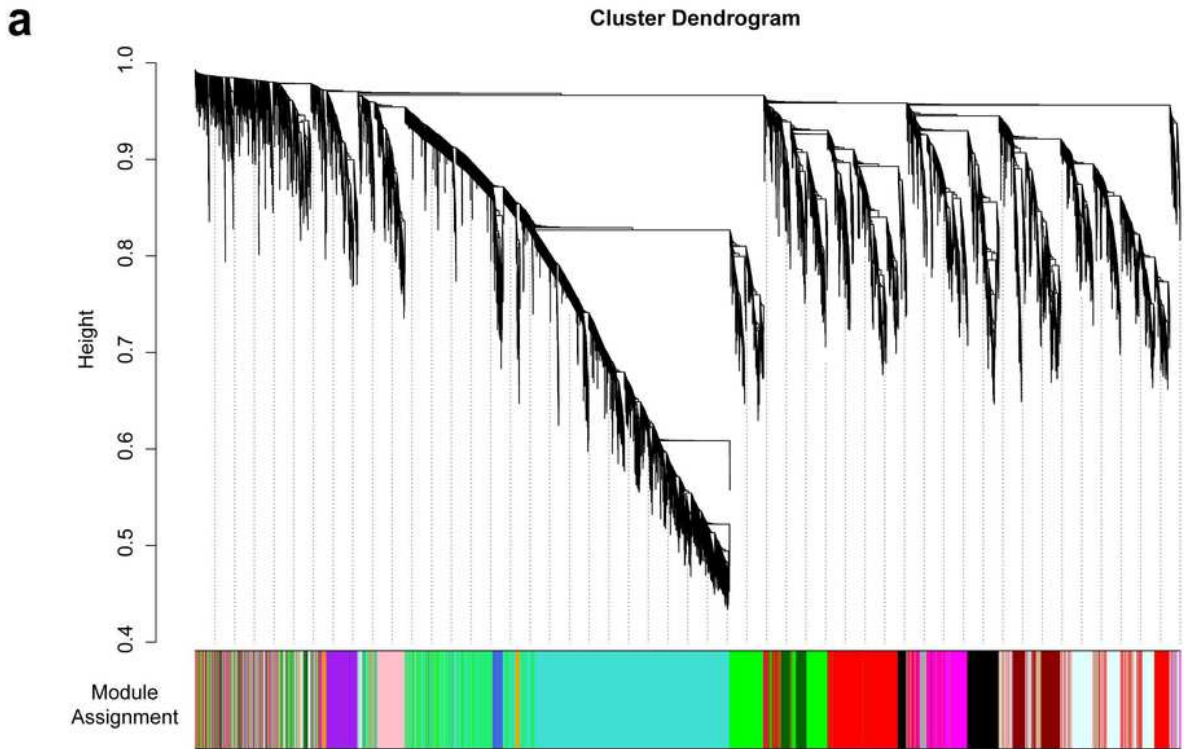


Figure 3

Identification of co expression genes related to candidate genes by Weighted gene co expression network analysis (WGCNA). a Hierarchical cluster tree showing the co expression modules identified by WGCNA. b The overlapped pathways that are enriched for gene modules turquoise and dark red.

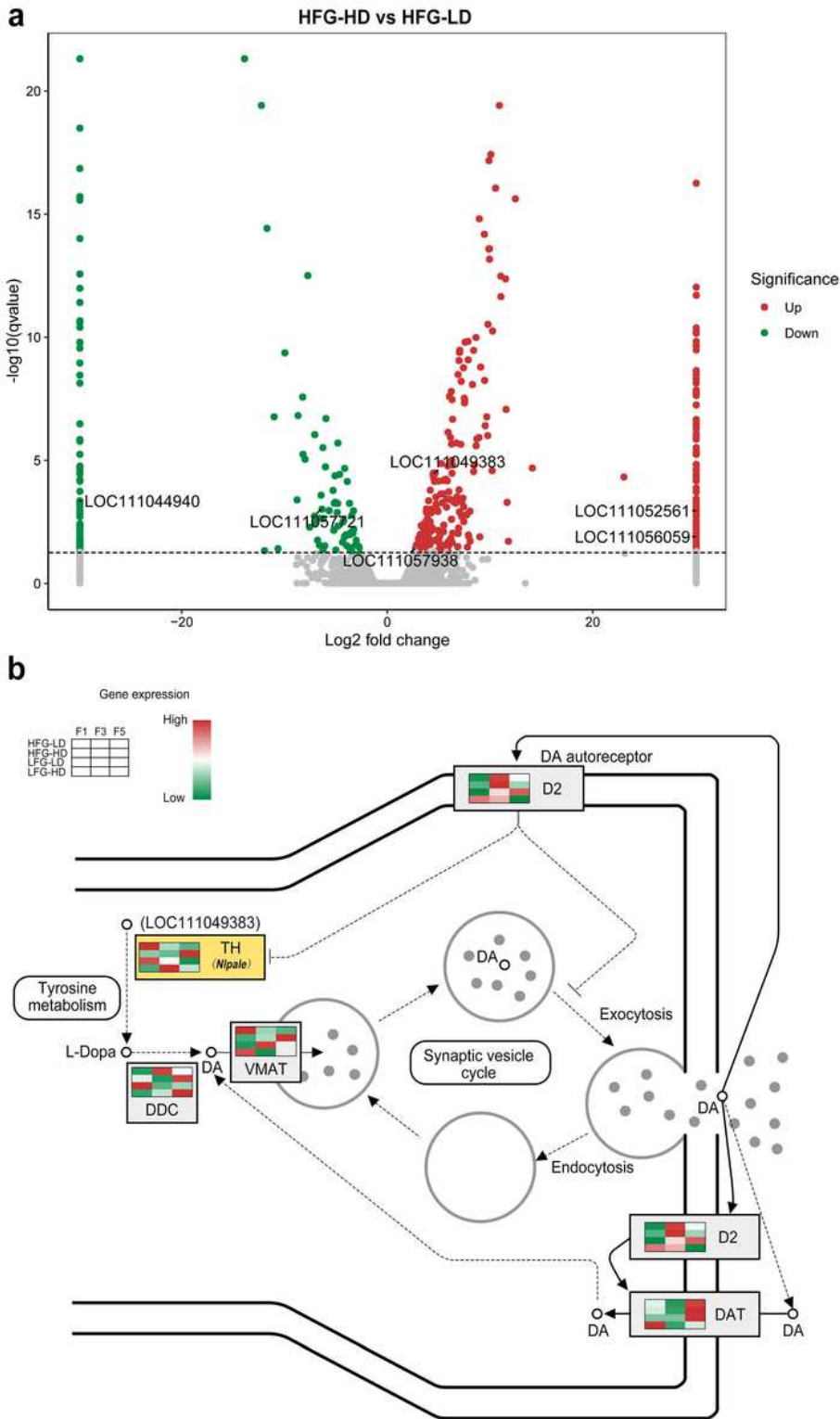


Figure 4

Targeting the key regulatory factors by differential expression analysis. a A volcano plot of the gene expression pattern between HFG HD and HFG LD at F5. The black, red and green points represent no difference in expression, up regulated genes and down regulated genes (FDR \leq 0.05, Benjamini and Hochberg adjustment). b The pathway map of Dopaminergic synapse. The expression patterns of detected genes in this pathway are presented by heatmap.

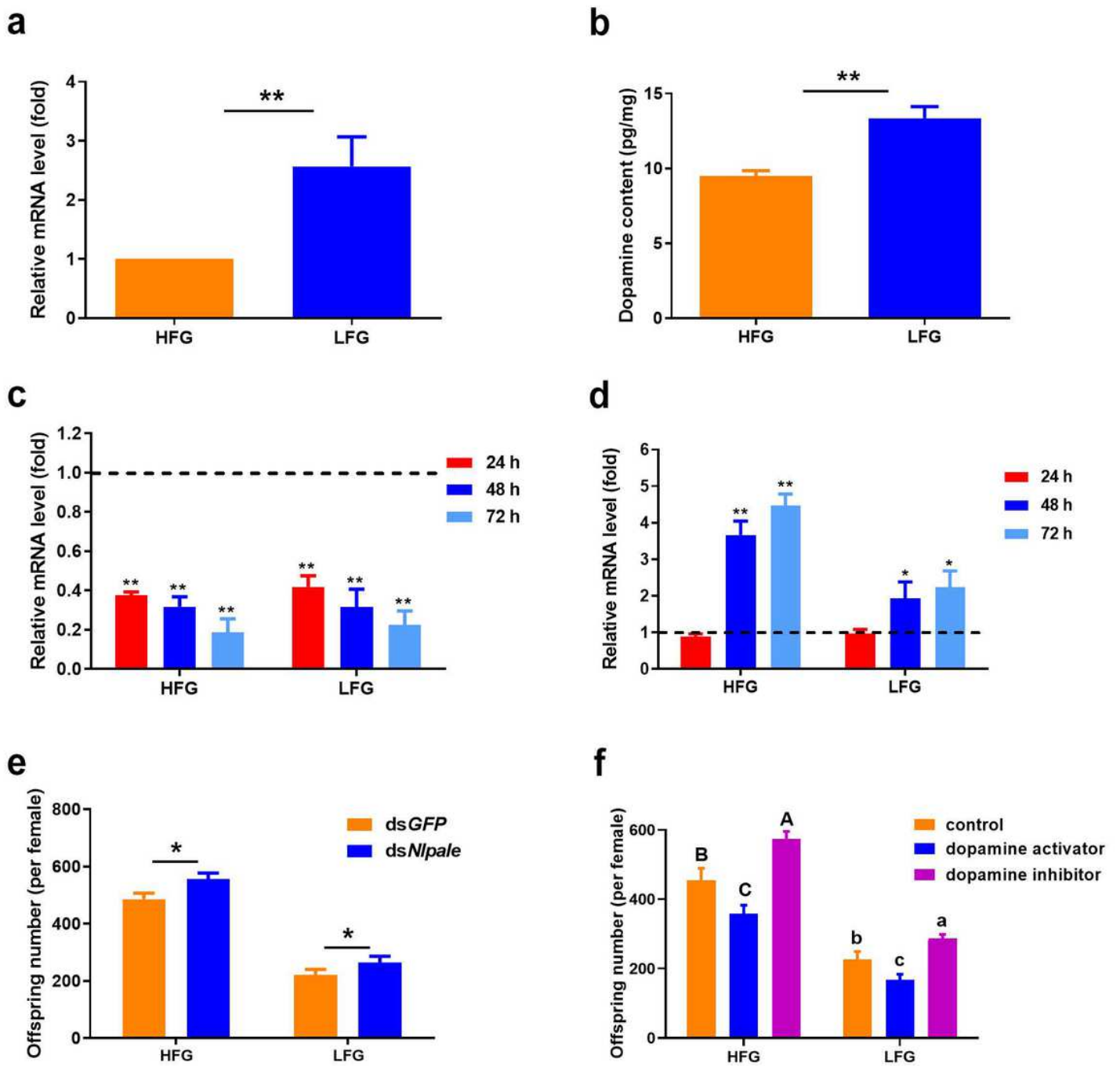


Figure 5

The role of Nlpale mRNA level and dopamine content in the fecundity of BPH. The Nlpale mRNA levels (a) and dopamine contents (b) in two genotypes insects are presented. The mRNA levels of Nlpale (c) and NIVg (d) in the two genotypes of BPH were measured at 24, 48 and 72 h after RNA interference of Nlpale. The insects injected with dsGFP were used as control. e The fecundity of HFG and LFG after injection of Nlpale dsRNA. f The fecundity of HFG and LFG after injection of dopamine inhibitor chlorpromazine, dopamine hydrochloride (activator), and water control. All data are presented as mean \pm SE. *: P < 0.05

level; **: $P < 0.01$ level (student's t test). The values sharing different letters are significantly different at $P < 0.05$ (one way ANOVA and Duncan's multiple range test).

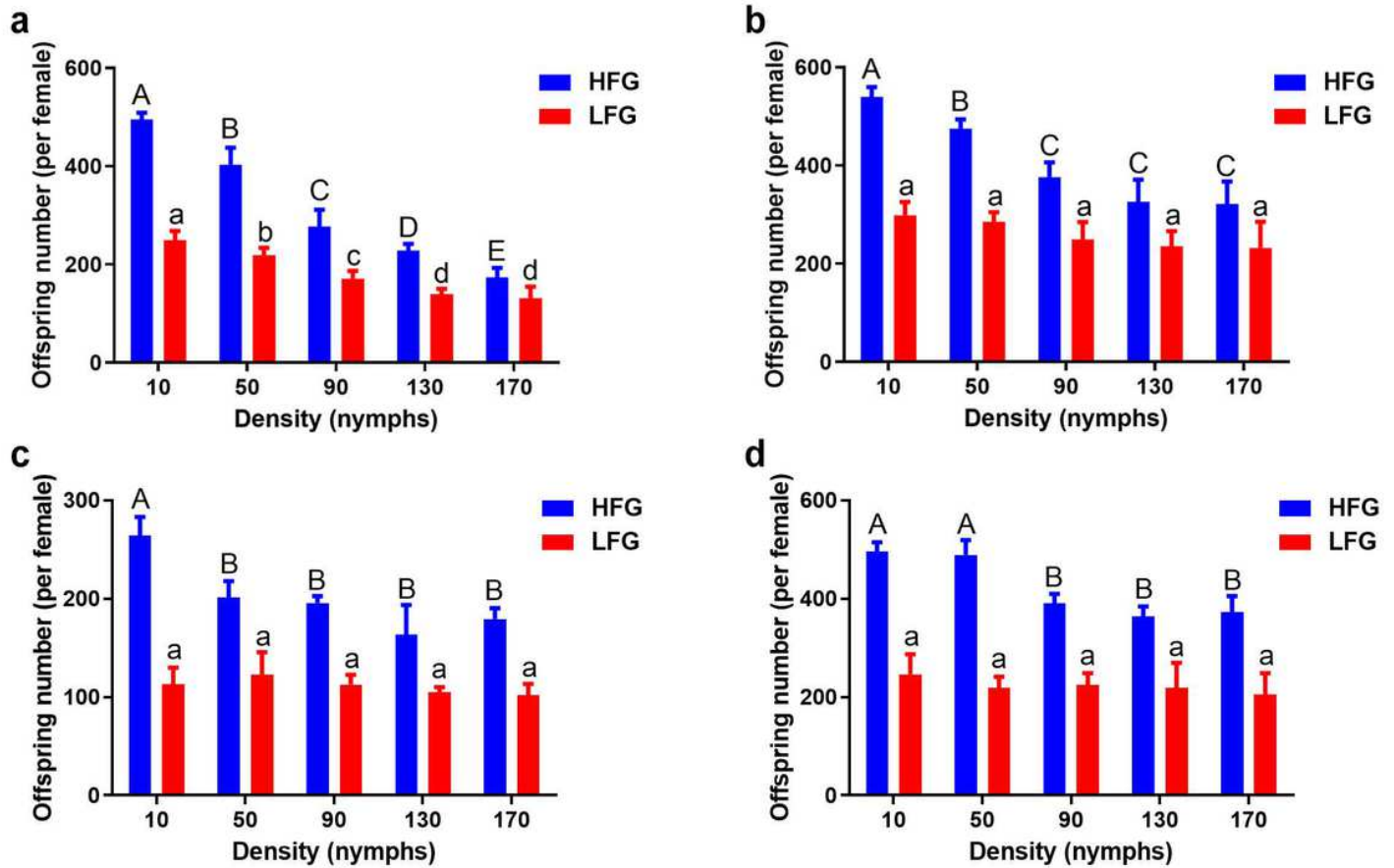


Figure 6

The role of dopamine biosynthesis in the density dependent effects on the fecundity of BPH. The impact of injection of dsGFP (a), dsNlpaIe (b), dopamine hydrochloride (c), and chlorpromazine (d) on the fecundity of two genotypes insects under the population densities of 10, 50, 90, 130 and 170 individuals. All data are presented as mean \pm SE. The values sharing different capital letters are significantly different at $P < 0.05$ within the HFG, and the values sharing different lowercase letter are significantly different at $P < 0.05$ within the LFG (one way ANOVA and Duncan's multiple range test).

Supplementary Files

This is a list of supplementary files associated with this preprint. Click to download.

- [FigS1.tif](#)
- [FigS2.tif](#)
- [TableS1.xlsx](#)
- [TableS2.xlsx](#)
- [TableS3.xlsx](#)

- [TableS4.xlsx](#)
- [TableS5.xlsx](#)
- [TableS6.xlsx](#)
- [TableS7.xlsx](#)
- [TableS8.xlsx](#)